f2 stock solution (see section on Bacteriophages) was placed on a 400-mesh copper grid with collodion membrane (Nissin EM Corp., Tokyo, Japan) and adsorbed onto the grid for 1 min. Excess solution was drained from the side of the grid with filter paper, and f1 or f2 was negatively stained with 10 μL of 2% phosphotungstic acid (pH 7.0) for 45 s. After the excess strain was drained off, the grid was examined with a transmission electron microscope (TEM, JEM-1210, Jeol Ltd, Tokyo, Japan).

Electrophoretic mobility

The electrophoretic mobility of bacteriophages was measured in prepared Milli-Q water and in filtered river water. Alkalinity was adjusted to 20 mg-$CaCO_3$/L with 0.4 mM $NaHCO_3$, and HCl was used to adjust the pH to 6.8. River water was filtered through a stirred ultrafiltration cell (Model 8400, Millipore Corp.) with an ultrafiltration membrane (molecular weight cutoff 100,000, regenerated cellulose; Ultrafiltration Disks, YM-100, Millipore Corp.) to exclude the large particles, and the pH was adjusted to 6.8 with HCl. The Milli-Q and river water samples were kept for 1 day at 20 °C to stabilize the pH. Just before the measurement of the electrophoretic mobility, bacteriophage stock solutions (see section on Bacteriophages) were used to suspend each bacteriophage at approximately 10^{10} PFU/mL in the prepared Milli-Q water or filtered river water. The electrophoretic mobility of the bacteriophages was measured 25 times for each sample at 25 °C and at a 15° measurement angle with an electrophoretic light-scattering spectrophotometer (ELS-6000, Otsuka Electronics Co., Ltd).

RESULTS AND DISCUSSION

Particle diameter and electrophoretic mobility

Figure 1 shows the electron micrographs of f1 and f2. Filamentous particles that were approximately 6–10 nm in diameter and 600–1,000 nm in length were observed for f1, whereas icosahedral particles approximately 25 nm in diameter were observed for f2. These particle characteristics are in agreement with previous reports (Shelton & Drewry 1973; Dotto *et al.* 1981). As seen in sandy aquifer treatment processes (Dowd *et al.* 1998), the differences in the particle sizes of f1 and f2 also probably influence their behavior during drinking water treatment processes.

Figure 2 shows a comparison in electrophoretic mobility (i.e. surface charge) between f1 and f2 in prepared Milli-Q water and filtered river water. When an electric field is applied to a suspension of charged particles, the particles move toward one of the electrodes. Negatively charged particles move toward the positive electrode and vice versa. The velocity of the particles is directly proportional to the applied field strength, and the ratio of these two quantities is known as the electrophoretic mobility (Gregory 2006). Accordingly, surface charge of particles can be evaluated by electrophoretic mobility measurements. Both bacteriophages were negatively charged in the prepared Milli-Q water, with f1 having a slightly more negative surface charge than f2. This difference in electrophoretic mobility is probably due to the differences in the types of amino acids (Weber & Konigsberg 1967; Beck & Zink 1981) on the surfaces of f1

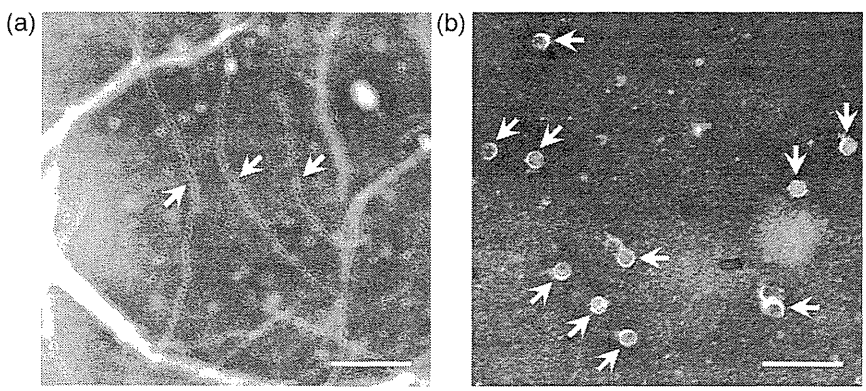

Figure 1 | Negative-stain electron micrographs of (a) f1 and (b) f2. The scale bar represents 100 nm.

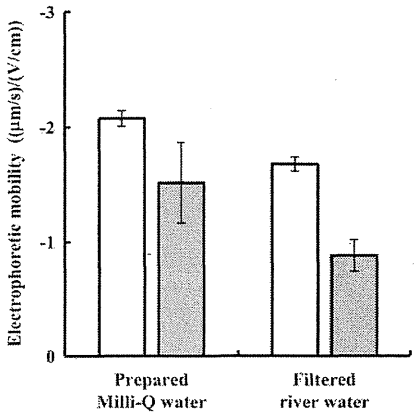

Figure 2 | Electrophoretic mobility of f1 (white) and f2 (gray) in prepared Milli-Q water and filtered river water. Values represent the mean and standard deviation of 25 measurements. The bacteriophage concentration in each sample was approximately 10^{10} PFU/mL.

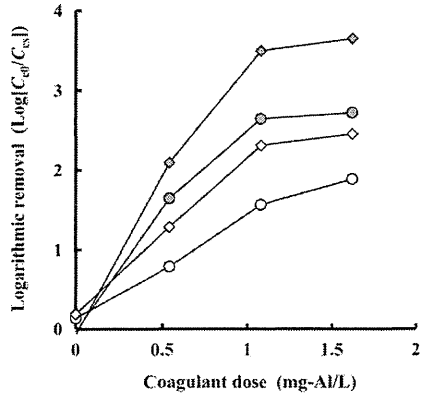

Figure 3 | Effects of coagulant dose (0.54, 1.08, or 1.62 mg-Al/L) on f1 (white) and f2 (gray) removal after settling, without (circles) or with (diamonds) centrifugal separation. The initial bacteriophage concentration in raw water was approximately 10^6 PFU/mL.

and f2. The same trend in electrophoretic mobility seen in prepared Milli-Q water was observed in filtered river water, although the electrophoretic mobility of both bacteriophages was shifted to the neutral owing to the differences in the ionic strength of the river water or to the influence of multivalent cations, such as calcium and magnesium ions. In general, the surface charge on virus particles strongly affects their behavior during various physicochemical water treatment processes, including coagulation processes (Matsushita *et al.* 2004). The more negatively charged viruses may resist aggregation, making it more difficult to destabilize and aggregate them by charge neutralization during coagulation in comparison to less negatively charged viruses. Thus, removal of f1 from river water by coagulation is expected to be more difficult than removal of f2.

Effects of coagulant dose on bacteriophage removal

Figure 3 shows the removal ratios, ($\log[C_{c0}/C_{cs}]$), for f1 and f2 after settling, with and without centrifugal separation, during coagulation. Because the diameters of f1 and f2 were small (as seen by electron microscopy) and they were stabilized by electrical repulsion in the river water, neither bacteriophage was removed (<0.2-log) from river water in the absence of coagulant. In contrast, both bacteriophages were removed by coagulation by the addition of any dose of the coagulant. The addition of coagulant destabilized the stably monodispersed bacteriophages in the river water, which got adsorbed onto/entrapped in the aluminium floc particles generated during coagulation. The aluminium floc particles were settled from suspension by gravity along with the adsorbed/entrapped bacteriophages during the settling process. Removal ratios of f1 and f2 were only approximately 1-log at 0.54 mg-Al/L of the coagulant, and the ratios increased to approximately 2-log with 1.08 mg-Al/L or more. Hijnen & Medema (2010) reviewed literature for viral removal performance in different coagulation processes (full-scale systems, pilot-plant studies and laboratory experiments) and estimated that the micro-organism elimination credit (MEC) of coagulation was 1.8±0.7-log for viruses (Hijnen & Medema 2010). Although the efficacy of coagulation for the removal of viruses is influenced by several conditions, such as raw water quality, the nature and concentrations of chemicals, pH, temperature and the type of mixing (Hijnen & Medema 2010), a similar removal performance (approximately 2-log) was observed for both bacteriophages in the present coagulation process.

The removal ratios of both bacteriophages increased after centrifugal separation. This indicates that centrifugal separation was able to remove the bacteriophages that were adsorbed onto/entrapped in the floc particles that were unable to settle by gravity.

However, regardless of centrifugal separation, the removal ratios of f1 were approximately 1-log lower than the ratio of f2 at any dose of the coagulant. This difference could be partly due to the difference in the electrophoretic

mobility of f1 and f2 in river water, as described above. Thus the removal of f1 from river water by coagulation was more difficult than that of f2.

Comparison of removal ratios of f1 and f2 during the coagulation–rapid sand filtration process

Figure 4 shows the removal ratios, ($\log[C_{c0}/C_{cs}]+\log[C_{r0}/C_{rf}]$), for f1 and f2 in the coagulation–rapid sand filtration process. Based on the results of the coagulation experiments, 1.08 mg-Al/L of coagulant was used in the coagulation–rapid sand filtration experiments. Although the DOC concentration of bacteriophage-spiked river water increased with the bacteriophage feed concentration, owing to the unavoidable uptake of the residual component of the culture medium, the removal ratios did not differ between initial concentrations of 10^6 and 10^8 PFU/mL for both bacteriophages (data not shown). This finding suggests that the DOC component from the bacteriophage culture solution did not affect bacteriophage removal during the coagulation process. Approximately 1-log improvement was seen in the removal ratios for f1 and f2 by the addition of the rapid sand filtration process in comparison to the coagulation process alone (Figure 3). This means that the bacteriophages entrapped in the suspended aluminium floc particles were effectively removed by the rapid sand filtration process after coagulation. In addition, no differences were observed in the removal ratios for f1 or f2 for filter depths of 10 and 20 cm. Thus, the effect of filter depth on bacteriophage removal was negligible, and most of the suspended aluminium floc particles were retained in the surface layer of the silica sand filter in the coagulation–rapid sand filtration process. Moreover, the removal ratios for both bacteriophages increased slightly with filtration time, which was probably due to the surface clogging of the silica sand filter by the deposition of suspended aluminium floc particles on the silica sand. In general, virus removal performance in the filtration process is increased with filtration time by pore clogging. In other words, the virus removal performance in the beginning of filtration time or just after the hydraulic backwashing can be regarded as a worst case scenario. Accordingly, the virus removal performances observed in the present study are assumed as their worst cases for elimination of virus in the filtration process since filtration time applied here is shorter than that of actual cases.

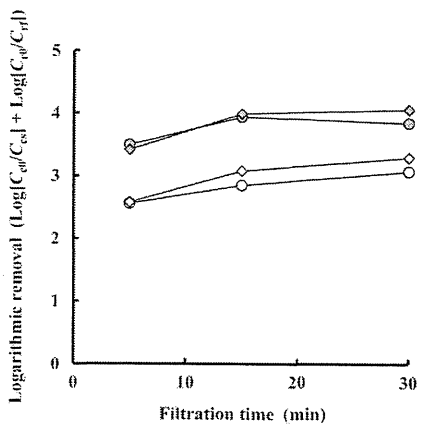

Figure 4 | Removal of f1 (white) and f2 (gray) by coagulation–rapid sand filtration with 10 cm (circles) or 20 cm (diamonds) of filter depth. The coagulant dose was 1.08 mg-Al/L. The initial bacteriophage concentration in raw water was approximately 10^8 PFU/mL.

Based on literature reports describing the viral removal performance by coagulation–rapid granular filtration processes, MEC was estimated to be 3.0±1.4-log for viruses (Hijnen & Medema 2010). A similar removal ratio of approximately 3–4-log was also observed for both bacteriophages after 30 min of filtration time in the present coagulation–rapid sand filtration process. However, the removal ratios of f1 were approximately 1-log lower than those of f2 for any duration of filtration. Thus, the behavior of both bacteriophages was different not only during the coagulation process but also in the coagulation–rapid sand filtration process.

Comparison of removal ratios of f1 and f2 during the coagulation–MF process

Figure 5 shows the removal ratios, ($\log[C_{c0}/C_{cs}]+\log[C_{m0}/C_{mf}]$), for f1 and f2 during the coagulation–MF process. Based on the results of the coagulation experiments, the coagulant dose used in the coagulation–MF experiments was 1.08 mg-Al/L. The coagulation–MF process effectively removed both bacteriophages: approximately 5-log increments were observed in the removal ratios for both bacteriophages by the addition of the MF process in comparison to the coagulation process alone (Figure 3), and time-averaged removal ratios of 5.6-log and 6.7-log were obtained for f1 and f2, respectively. This indicates that almost all suspended aluminium floc particles with adsorbed/entrapped bacteriophages exceeded the pore size of

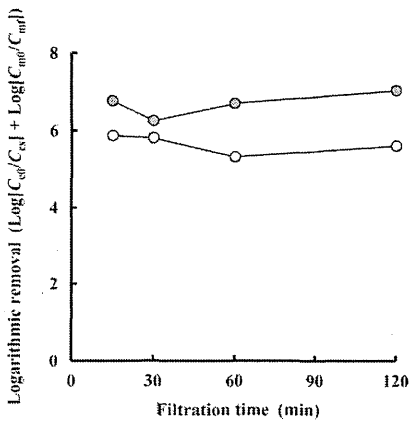

Figure 5 | *Removal of f1 (white) and f2 (gray) by coagulation–MF. The coagulant dose was 1.08 mg-Al/L. The initial bacteriophage concentration in raw water was approximately 10^8 PFU/mL.*

the MF membrane and were removed by the MF process. Other researchers have also demonstrated the effectiveness of the coagulation–MF process: virus removal ratios of >4-log were achieved by the combination of aluminium/iron-based coagulation and organic/inorganic MF processes (Matsushita *et al.* 2005; Zhu *et al.* 2005; Fiksdal & Leiknes 2006).

The removal ratios for both bacteriophages were almost constant during filtration. In contrast, removal ratios for the F-specific RNA bacteriophages Qβ and MS2 gradually increased with filtration time in an in-line coagulation–MF process, probably due to the accumulation of (i) a cake layer on the membrane surface and (ii) viruses as irreversible foulants in the internal structure of the membrane pores (Shirasaki *et al.* 2009). One reason for this discrepancy is the difference in the coagulation processes (batch coagulation vs. in-line coagulation): most of the aluminium floc particles generated during the coagulation process were settled out from the suspension by gravity, and the floc particles remaining in the supernatant were fed into the MF membrane in the batch coagulation process. On the other hand, almost all the floc particles generated were fed into the MF membrane in the in-line coagulation process. Thus, the effects of the cake layer and of the irreversible foulants on bacteriophage removal during batch and in-line coagulation were quite different, leading to the differences in the trends of the removal ratios for bacteriophages.

As seen in the coagulation and coagulation–rapid sand filtration processes, the removal ratios for f1 were approximately 1-log lower than those for f2 for any duration of filtration during the coagulation–MF process. Thus, the removal of f1 by the combination of coagulation and filtration processes is more difficult than that of f2 from river water.

The US Environmental Protection Agency (USEPA) National Primary Drinking Water Standards (US Environmental Protection Agency 2001) require 4-log removal or inactivation of enteric viruses from source water by filtration, disinfection or a combination of these technologies. This 4-log removal was achieved in the present study by the coagulation–MF process, regardless of bacteriophage characteristics (filamentous vs. spherical). Thus, the coagulation–MF process is effective for the removal of both filamentous and spherical viruses, and has the potential to effectively mitigate the public health risk posed by virus contamination in drinking water.

CONCLUSIONS

1. The removal performances of coagulation, coagulation–rapid sand filtration, and coagulation–MF processes were different for f1 and f2: the removal ratios for f1 were approximately 1-log lower than those for f2, probably due to the differences in the particle characteristics and the surface charges of f1 and f2.
2. The coagulation–MF process was more effective than the coagulation–rapid sand filtration process for the removal of both bacteriophages: the removal ratios for f1 and f2 in the coagulation–MF process were approximately 6-log and 7-log, respectively, and these values were approximately 3-log higher than those observed for the coagulation–rapid sand filtration process.
3. The public health risk posed by virus contamination in drinking water will be effectively mitigated by the replacement of the coagulation–rapid sand filtration process with the coagulation–MF process.

ACKNOWLEDGEMENTS

We thank Norikazu Isoda (Department of Disease Control, Graduate School of Veterinary Medicine, Hokkaido University), who instructed us in the methods of electron

microscopic analysis. This research was supported in part by a Grant-in-Aid for the Encouragement of Young Scientists (no. 21686049, 2009) from the Ministry of Education, Culture, Sports, Science and Technology of Japan, and a Grant-in-Aid (no. 71250001, 2010) from Ministry of Health, Labor and Welfare of Japan.

REFERENCES

Adams, M. H. 1959 *Bacteriophages*. Interscience Publishers, New York, NY, USA, pp. 450–454.

Beck, E. & Zink, B. 1981 Nucleotide sequence and genome organisation of filamentous bacteriophages f1 and fd. *Gene* **16** (1–3), 35–58.

Cole, D., Long, S. C. & Sobsey, M. D. 2003 Evaluation of F+ RNA and DNA coliphages as source-specific indicators of fecal contamination in surface waters. *Appl. Environ. Microbiol.* **69** (11), 6507–6514.

Dotto, G. P., Enea, V. & Zinder, N. D. 1981 Gene II of phage f1: its functions and its products. *Proc. Natl. Acad. Sci. USA* **78** (9), 5421–5424.

Dowd, S. E., Pillai, S. D., Wang, S. & Corapcioglu, M. Y. 1998 Delineating the specific influence of virus isoelectric point and size on virus adsorption and transport through sandy soils. *Appl. Environ. Microbiol.* **64** (2), 405–410.

Fauquet, C. M., Mayo, M. A., Maniloff, J., Desselberger, U. & Ball, L. A. (eds). 2005 *Virus Taxonomy: Eighth report of the International Committee on Taxonomy of Viruses*. Elsevier Academic Press, London, UK, pp. 279–287, 741–750.

Fiksdal, L. & Leiknes, T. O. 2006 The effect of coagulation with MF/UF membrane filtration for the removal of virus in drinking water. *J. Membr. Sci.* **279** (1–2), 364–371.

Gregory, J. 2006 *Particles in Water: Properties and Processes*. IWA Publishing, London, UK, 60pp.

Guillot, E. & Loret, J. F. 2010 *Waterborne Pathogens: Review for the Drinking Water Industry*. IWA Publishing, London, UK.

Haramoto, E., Kitajima, M., Katayama, H., Asami, M., Akiba, M. & Kunikane, S. 2009 Application of real-time PCR assays to genotyping of F-specific phages in river water and sediments in Japan. *Water Res.* **43** (15), 3759–3764.

Havelaar, A. H., Olphen, M. & Drost, Y. C. 1993 F-specific RNA bacteriophages are adequate model organisms for enteric viruses in fresh water. *Appl. Environ. Microbiol.* **59** (9), 2956–2962.

Hijnen, W. A. M. & Medema, G. J. 2010 *Elimination of Micro-organisms by Water Treatment Processes*. IWA Publishing, London, UK, pp. 9–10, 23–34.

Long, S. C. & Sobsey, M. D. 2004 A comparison of the survival of F+ RNA and F+ DNA coliphages in lake water microcosms. *J. Water Health* **2** (1), 15–22.

Matsushita, T., Matsui, Y. & Inoue, T. 2004 Irreversible and reversible adhesions between virus particles and hydrolyzing precipitating aluminum: a function of coagulation. *Water Sci. Technol.* **50** (12), 201–206.

Matsushita, T., Matsui, Y., Shirasaki, N. & Kato, Y. 2005 Effect of membrane pore size, coagulation time, and coagulant dose on virus removal by a coagulation-ceramic microfiltration hybrid system. *Desalination* **178** (1–3), 21–26.

Nappier, S. P., Aitken, M. D. & Sobsey, M. D. 2006 Male-specific coliphages as indicators of thermal inactivation of pathogens in biosolids. *Appl. Environ. Microbiol.* **72** (4), 2471–2475.

Payment, P., Trudel, M. & Plante, R. 1985 Elimination of viruses and indicator bacteria at each step of treatment during preparation of drinking water at seven water treatment plants. *Appl. Environ. Microbiol.* **49** (6), 1418–1428.

Pierre, G., Causserand, C., Roques, C. & Aimar, P. 2010 Adsorption of MS2 bacteriophage on ultrafiltration membrane laboratory equipments. *Desalination* **250** (2), 762–766.

Redman, J. A., Grant, S. B., Olson, T. M., Adkins, J. M., Jackson, J. L., Castillo, M. S. & Yanko, W. A. 1999 Physicochemical mechanisms responsible for the filtration and mobilization of a filamentous bacteriophage in quartz sand. *Water Res.* **33** (1), 43–52.

Shelton, S. P. & Drewry, W. A. 1973 Tests for coagulants for the reduction of viruses, turbidity, and chemical oxygen demand. *J. Am. Water Work Assoc.* **65** (10), 627–635.

Shirasaki, N., Matsushita, T., Matsui, Y., Kobuke, M. & Ohno, K. 2009 Comparison of removal performance of two surrogates for pathogenic waterborne viruses, bacteriophage Qβ and MS2, in a coagulation–ceramic microfiltration system. *J. Membr. Sci.* **326** (2), 564–571.

Stetler, R. E. 1984 Coliphages as indicators of enteroviruses. *Appl. Environ. Microbiol.* **48** (3), 668–670.

US Environmental Protection Agency 2001 *National Primary Drinking Water Standards*. Office of Water, US Environmental Protection Agency, Washington, DC, EPA816-F-01-007.

Waldor, M. K. & Mekalanos, J. J. 1996 Lysogenic conversion by a filamentous phage encoding cholera toxin. *Science* **272** (5270), 1910–1914.

Weber, K. & Konigsberg, W. 1967 Amino acid sequence of the f2 coat protein. *J. Biol. Chem.* **242** (15), 3563–3578.

World Health Organization 2008 *Guidelines for Drinking-Water Quality: Third ed., Incorporating the First and Second Addenda, Vol.1-Recommendations*. World Health Organization, Geneva, Switzerland, pp. 289–292.

Zhu, B., Clifford, D. A. & Chellam, S. 2005 Virus removal by iron coagulation-microfiltration. *Water Res.* **39** (20), 5153–5161.

First received 25 November 2011; accepted in revised form 13 April 2012

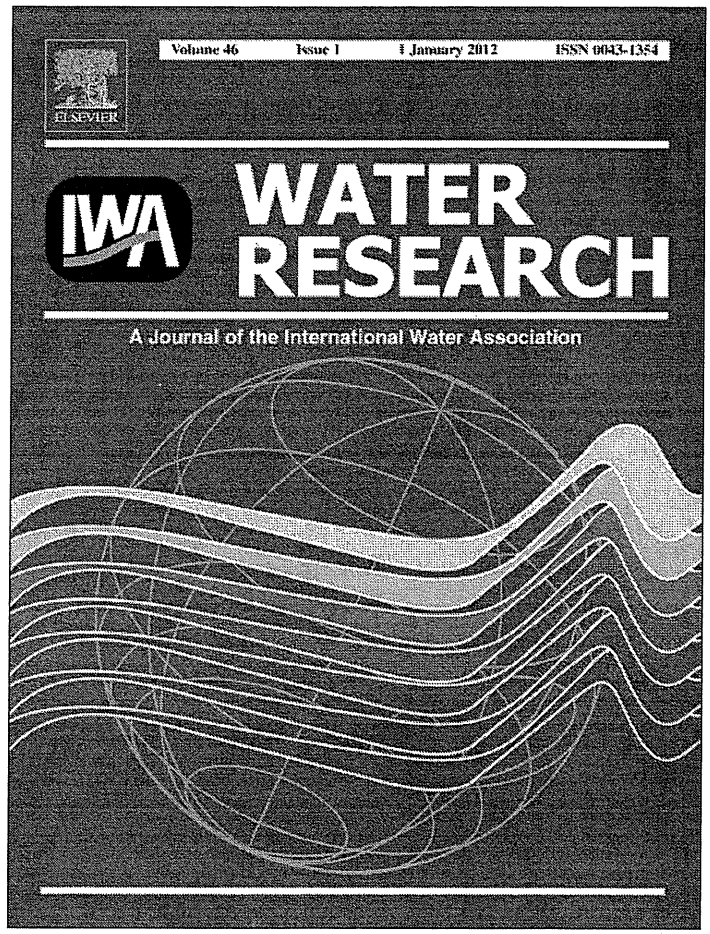

WATER RESEARCH 46 (2012) 187–194

Available online at www.sciencedirect.com

SciVerse ScienceDirect

journal homepage: www.elsevier.com/locate/watres

Quantitative detection of *Cryptosporidium* oocyst in water source based on 18S rRNA by alternately binding probe competitive reverse transcription polymerase chain reaction (ABC-RT-PCR)

Naohiro Kishida [a,*], *Ryo Miyata* [b], *Atsushi Furuta* [b,c], *Shinji Izumiyama* [d], *Satoshi Tsuneda* [c], *Yuji Sekiguchi* [b], *Naohiro Noda* [b], *Michihiro Akiba* [a]

[a] *Division of Water Management, Department of Environmental Health, National Institute of Public Health, 2-3-6 Minami, Wako, Saitama 351 0197, Japan*

[b] *Biomedical Research Institute, National Institute of Advanced Industrial Science and Technology (AIST), Central 6, Higashi 1-1-1, Tsukuba, Ibaraki 305 8566, Japan*

[c] *Department of Life Science and Medical Bioscience, Waseda University, 2-2 Wakamatsu-cho, Shinjuku-ku, Tokyo 162 8480, Japan*

[d] *Department of Parasitology, National Institute of Infectious Diseases, Toyama 1-23-1, Shinjuku, Tokyo 162 8640, Japan*

ARTICLE INFO

Article history:
Received 11 August 2011
Received in revised form
19 October 2011
Accepted 21 October 2011
Available online 29 October 2011

Keywords:
Cryptosporidiosis
Fluorescence quenching
Health-related water microbiology
Real-time PCR

ABSTRACT

We describe an assay for simple and cost-effective quantification of *Cryptosporidium* oocysts in water samples using a recently developed quantification method named alternately binding probe competitive PCR (ABC-PCR). The assay is based on the detection of 18S rRNA specific for *Cryptosporidium* oocysts. The standard curve of the ABC-PCR assay had a good fitting to a rectangular hyperbola with a correlation coefficient (*R*) of 0.9997. Concentrations of *Cryptosporidium* oocysts in real river water samples were successfully quantified by the ABC-reverse transcription (RT)-PCR assay. The quantified values by the ABC-RT-PCR assay very closely resemble those by the real-time RT-PCR assay. In addition, the quantified concentration in most water samples by the ABC-RT-PCR assay was comparable to that by conventional microscopic observation. Thus, *Cryptosporidium* oocysts in water samples can be accurately and specifically determined by the ABC-RT-PCR assay. As the only equipment that is needed for this end-point fluorescence assay is a simple fluorometer and a relatively inexpensive thermal cycler, this method can markedly reduce time and cost to quantify *Cryptosporidium* oocysts and other health-related water microorganisms.

1. Introduction

Members of the genus *Cryptosporidium* are protozoan parasites that can cause the gastrointestinal disease cryptosporidiosis (O'Donoghue, 1995). Cryptosporidiosis remains a public health concern, as demonstrated by continued outbreaks of this disease (Nichols, 2008). Waterborne cryptosporidiosis is particularly important because *Cryptosporidium* oocysts are resistant to disinfectants such as chlorine commonly used for water treatment (Peeters et al., 1989; Carpenter et al., 1999).

* *Corresponding author.* Tel.: +81 48 458 6274; fax: +81 48 458 6275.
E-mail address: kishida@niph.go.jp (N. Kishida).

0043-1354/$ – see front matter © 2011 Elsevier Ltd. All rights reserved.
doi:10.1016/j.watres.2011.10.048

Detection of *Cryptosporidium* oocysts in water samples has been carried out by direct microscopic visualization or enzyme immunoassays of obtained and/or cultured oocysts with or without fluorescent antibodies. However, these detection methods are labor-intensive, require a large number of oocysts for positive detection and are not suitable for high-throughput processing of samples (Ramirez and Sreevatsan, 2006). Instead of these conventional methods, molecular (nucleic acid-based) techniques have been developed for rapid detection of *Cryptosporidium* oocysts from water samples. In particular, real-time polymerase chain reaction (PCR) is widely used for the quantification of *Cryptosporidium* oocysts (Keegan et al., 2003; King et al., 2005; Miller et al., 2006; Garcés-Sanchez et al., 2009) because of its high rapidity, sensitivity and reproducibility. However, the real-time PCR requires highly specialized and expensive devices that combine a fluorometer and a thermal cycler for real-time fluorescence measurement. Therefore, other simpler molecular quantification techniques are strongly needed for the routine detection of *Cryptosporidium* oocysts in drinking water treatment plants, bathing facilities, and wherever water quality monitoring is needed.

In this study, we focused our attention on a recently reported novel molecular method for the quantification of nucleic acid sequences named alternately binding probe competitive PCR (ABC-PCR) (Tani et al., 2007) as an improved method for quantification of *Cryptosporidium* oocysts. This method is cost-effective because it does not require an expensive real-time fluorescence measurement device but requires a simple end-point fluorescence measurement device. We developed this ABC-reverse transcription (RT)-PCR assay for cost-effective quantification of *Cryptosporidium* oocysts, and applied the assay to the detection from real water samples collected from Japanese rivers. To investigate the validity of the ABC-RT-PCR assay, real-time RT-PCR assay and conventional microscopic observation were also performed, and quantification data were compared with each other.

2. Principle and characteristics of ABC-PCR

The principle of ABC-PCR is as follows: the alternately binding probe (hereafter called "ABProbe") is labeled at the 5′ end with a green dye (BODIPY FL) and at the 3′ end with a red dye (6-carboxytetramethylrhodamine [TAMRA]) as shown in Fig. 1. These fluorescent dyes have a property of being notably quenched by an electron transfer to guanine at a particular position (Kurata et al., 2001; Torimura et al., 2001), and the green dye is quenched via the fluorescence resonance energy transfer (FRET) to the red dye when two fluorescent dyes are in proximity. The ABProbe hybridizes with the target and competitor in perfect match. The green fluorescence intensity reflects the ratio of the target and competitor (internal standard) DNAs, and the red fluorescence intensity reflects the ratio of the hybridized probe to the unbound probe. At the normal PCR using a thermal cycler, the target and competitor DNAs are coamplified with the same efficiency in the presence of the ABProbe. The number of copies of the target DNA can be calculated from the fluorescence intensity of the ABProbe at the end-point of PCR. Therefore, this method does not require expensive real-time fluorescence measurement device, but only requires end-point fluorescence measurement using a simple fluorometer, so that the measurement cost can be markedly reduced. Moreover, false-negative results can be easily confirmed by measuring the fluorescence intensity of red dye at the end-point of PCR, because the intensity does not change if PCR reaction itself does not proceed and therefore neither target nor competitor DNAs are amplified.

3. Materials and methods

3.1. *Sample collection and pretreatment*

In total, 14 water samples were collected at 7 sites in tributary rivers of the Tone River basin in Japan where the surface water is utilized for the main production of drinking water for people living in the Tokyo metropolitan area from November to December 2009. Ten liters of water samples were concentrated by vacuum filtration with polytetrafluoroethylene membrane filters (pore size: 1 μm; diameter: 142 mm, Advantec Toyo, Tokyo, Japan), and concentrated samples were eluted from the filter using a vortex mixer (Oda et al., 2002). Then they were purified through immunomagnetic separation (Dynabeads GC Combo, Life Technologies, California, USA). While the manufacturer recommended using 50 μL of 0.1 N HCl in the oocyst dissociation step, in our investigation the step was repeated once more to recover the oocysts. The neutralization procedure was performed in a 1.5 mL tube with 10 μL of 1 N NaOH. The final volume of concentrated sample solution was 110 μL. Half the volume of concentrated sample solution was used for the ABC-PCR and real-time PCR assays after nucleic acid extraction and reverse transcription, and the other half volume was used for a conventional assay based on microscopic observation.

3.2. *RNA extraction and reverse transcription*

Immediately after five freeze (−80 °C) and thaw (37 °C) cycles, the sample solution including *Cryptosporidium* oocysts was incubated at 60 °C for 30 min using a heat block with the solution for nucleic acids extraction containing 10 mM Tris (tris-hydroxymethyl-aminomethane)-HCl (pH 7.6), 1 mM EDTA (ethylenediaminetetraacetic acid), 2 mM NaCl, 0.1% TritonX-100 (t-octylphenoxy-polyethoxyethanol), 2 mM DTT (dithiothreitol) and 1.5 mAnson-U/mL Proteinase K. The sample solution was sonicated for 2 min and incubated at 75 °C for 10 min. Then the solution was incubated at 95 °C for 5 min to deactivate Proteinase K, and immediately cooled down on ice. Next, extracted RNA solution was subjected to reverse transcription using PrimeScript RT reagent Kit (Takara Bio, Shiga, Japan) with 2.5 μM of Crypt-374r primer shown in Table 1 to obtain cDNA. The reverse transcription reaction was performed using GeneAmp PCR system 9700 (Life Technologies, California, USA) with the following program: reverse transcription at 37 °C for 15 min and inactivation of enzyme at 85 °C for 5 s. Synthesized cDNA was used as template DNA in the ABC-PCR and real-time PCR assays.

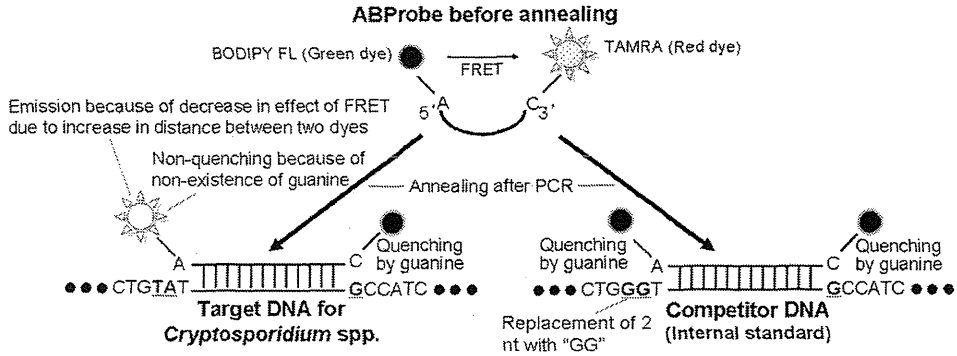

Fig. 1 – Schematic presentation of a novel ABC-PCR assay for calculating the ratio of the target to the competitor in competitive PCR. The target shown here is an example that possesses a T base at the 3′ end of the probe binding site; however, the presence of A is also acceptable in this method. The competitor has the same sequence as the target, except that the underlined TA bases are replaced by GG bases. Fluorescence intensities reflect the ratio of target to competitor.

3.3. *Oligonucleotide sequences*

The sequences of primers and probes of the ABC-PCR and real-time PCR assays for the quantification of 18S rRNA of *Cryptosporidium* spp. are listed in Table 1. Primers with the same sequences were used for the ABC-PCR and real-time PCR assays, while the sequences of the ABProbe and TaqMan probe were a little different. A sequence of ABProbe was newly designed based on the sequence of the TaqMan probe used for the real-time PCR assay. The position of binding the ABProbe with 18S rRNA genes of *Cryptosporidium* spp. is displaced by 2 nt as shown in Table 1, because the nucleotide of ABProbe at the 3′ end must be cytosine in order to quench the red fluorescence (TAMRA) as shown in Fig. 1. Specificity of real-time PCR and ABC-PCR assays was confirmed in silico predictions using a basic local alignment search tool (Altschul et al., 1990).

The chemically synthesized oligo-DNA with a length of 192 bp was used for standard DNA for the ABC-PCR and real-time PCR assays. The sequence of the standard DNA was a partial sequence of the 18S rRNA genes of *Cryptosporidium hominis* (Accession No. AF093489; nucleotide position: 188–379). The internal standard (competitor) DNA was also chemically synthesized. The sequence of the internal standard DNA was different from the standard DNA sequence by 2 nt, i.e., AT to GG at the outside of the 5′ end position at which the ABProbe annealed (nucleotide position: 272–273) in order to quench the green fluorescence (BODIPY FL) only when the ABProbe is annealed to the sequence of the internal standard DNA, as shown in Fig. 1.

3.4. *ABC-PCR assay*

The PCR mixture (20 μL) consisted of 0.4 μL of 50 × TITANIUM Taq polymerase (Takara Bio, Tokyo, Japan), 2.0 μL of 10 × TITANIUM buffer, 200 μM each of dATP, dCTP and dGTP, 600 μM dUTP (Roche Diagnostics Japan, Tokyo, Japan), 0.25 unit of uracil-DNA glycosylase (heat-labile; Roche Diagnostics Japan, Tokyo, Japan), 75 nM Crypt-193f, 250 nM Crypt-374r, 200 nM Crypt-274Abp, 1 μL of competitor DNA (internal standard) and 1 μL of standard DNA or cDNA from water samples. PCR amplification was performed using Mastercycler (Eppendorf, Hamburg, Germany) with the following program: an initial denaturation at 95 °C for 2 min, 50 cycles of denaturation at 95 °C for 20 s, annealing at 60 °C for 20 s, extension at 72 °C for 20 s and final extension at 72 °C for 2 min. After the PCR amplification, the fluorescence intensity of each aliquot was measured at 95 and 60 °C using Light Cycler 480 (Roche

Table 1 – Nucleotide sequences of PCR primers and probes used to detect *Cryptosporidium* spp.

Name	Sequence (5′ → 3′)	Location[a]	Used for	References
Primer				
Crypt-193f	GGAAGGGTTGTATTTATTAGATAAAGAACCA	193	Real-time PCR and ABC-PCR	Miller et al., 2006
Crypt-374r	CTCCCTCTCCGGAATCGAA	374	Real-time PCR, ABC-PCR and reverse transcription	
TaqMan Probe				
Crypt-276p[b]	CATTCAAGTTTCTGACCTATCAGCTTTAGACGG	276	Real-time PCR	Miller et al., 2006
ABProbe				
Crypt-274Abp[c]	ATCATTCAAGTTTCTGACCTATCAGCTTTAGAC	274	ABC-PCR	This study

a Corresponding nucleotide position of *Cryptosporidium hominis* 18S rRNA gene (Accession No. AF093489) of the 5′ end.
b TaqMan probe oligonucleotides were labeled with 6-FAM at the 5′ end and BHQ at the 3′ end.
c Alternatively binding competitive probe oligonucleotides were labeled with BODIPY FL at the 5′ end and TAMRA at the 3′ end.

Diagnostics Japan, Tokyo, Japan). Excitation was performed at 450–495 and 522–555 nm, with 505–537 and 565–605 nm emission filters for green fluorescence and red fluorescence, respectively. Although a real-time fluorescence measurement device was used in order to analyze the fluorescence intensity at the end-point of PCR quickly in this study, a simple fluorometer can be also used for the same accuracy as has been reported in previous papers (Tani et al., 2007; Noda et al., 2008). Serial dilutions of the standard DNA (range: 10^1–10^5 copies per reaction) were used to make a standard curve. In addition, internal standard DNA with the concentration of 10^3 copies were added to each PCR mixture.

3.5. Data analysis of ABC-PCR assay

As shown in Fig. 1, the fluorescence intensity of the ABProbe changes as follows: (i) When the ABProbe is free in solution, its green fluorescence (G1) is notably quenched by FRET to the red dye. (ii) When the ABProbe hybridizes with a target, its green fluorescence (G2) is bright because the two fluorescent dyes are separate. (iii) When the ABProbe hybridizes with a competitor (internal standard), its green fluorescence (G3) is darker than G2 because its green fluorescence is quenched by guanine bases. (iv) When the ABProbe is free in solution, its red fluorescence (R1) is bright. (v) When the ABProbe hybridizes with the target or competitor, its red fluorescence is similarly quenched by the guanine complementary to the modified cytosine (R2 = R3). Therefore, the red fluorescence intensity reflects the ratio of the unbound probe to the hybridized probe, and the green fluorescence intensity reflects the ratio of target to the competitor in the PCR products. The fluorescence intensities of the green dye (G_{60}) and red dye (R_{60}) at 60 °C represent the intensity after hybridization, whereas those of the green dye (G_{95}) and red dye (R_{95}) at 95 °C represent the intensity before hybridization. These fluorescence intensities fluctuate slightly from tube to tube because of differences in the reagent volume and/or unknown factors. Therefore, G_{60} and R_{60} were divided by G_{95} and R_{95} to normalize the non-PCR-related fluorescence fluctuations occurring from tube to tube. The fluorescence intensities measured from the green dye (G_{60}/G_{95}) and red dye (R_{60}/R_{95}) are the sum of the fluorescence intensities from the unbound probe (G_U or R_U), the hybridized probe with the target (G_T or R_T), and the hybridized probe with the competitor (G_C or R_C), expressed, respectively, as

$$G_{60}/G_{95} = G_U(1-y) + G_T[X/(X+C)]y + G_C[C/(X+C)]y, \quad (1)$$

where y is the ratio of the bound probe to the total probe, and

$$R_{60}/R_{95} = R_U(1-y) + R_T[X/(X+C)]y + R_C[C/(X+C)]y. \quad (2)$$

X and C are the starting quantities of the target and competitor, respectively. At this point,

$$R_T = R_C. \quad (3)$$

Therefore, Eq. (2) converts to

$$y = [R_U - (R_{60}/R_{95})]/(R_U - R_C). \quad (4)$$

Under this condition, Eq. (1) converts to

$$[(G_{60}/G_{95}) - G_U]/[R_U - (R_{60}/R_{95})] = [(CG_C - CG_T)/(R_U - R_C)]/ \times (X+C) + (G_T - G_U)/ \times (R_U - R_C). \quad (5)$$

This equation shows that $[(G_{60}/G_{95}) - G_U]/[R_U - (R_{60}/R_{95})]$ and X have a relationship indicated by a rectangular hyperbola. Therefore, the standard curves were obtained by fitting the data points to a rectangular hyperbola, and the number of copies of 18S rRNA of *Cryptosporidium* spp. in each sample was calculated using the standard curves.

3.6. Real-time PCR assay

The PCR mixture (20 μL) consisted of 400 nM of each primer, 80 nM of the TaqMan probe, commercially available PCR mastermix (LightCycler FastStart DNA Master^{PLUS} HybProbe; Roche Diagnostics Japan, Tokyo, Japan) and 2 μL of standard DNA or cDNA from water samples. PCR amplification and fluorescence measurement was performed using LightCycler 2.0 (Roche Diagnostics Japan, Tokyo, Japan) with the following program: an initial denaturation at 95 °C for 10 min, 50 cycles of denaturation at 95 °C for 10 s, annealing and extension at 60 °C for 30 s. Crossing point (Cp) values were determined automatically by LightCycler software using the second derivative maximum method.

3.7. Conversion of number of 18S rRNA molecules of Cryptosporidium spp. to number of Cryptosporidium oocysts

The number of 18S rRNA molecules in a standard *Cryptosporidium* oocyst was investigated by real-time RT-PCR, and the number was used for conversion of the number of copies of 18S rRNA molecules in water samples as determined by the ABC-RT-PCR and real-time RT-PCR assays to the number of *Cryptosporidium* oocysts. *Cryptosporidium parvum* oocysts (H8 strain, Yagita et al., 2001) which were maintained in our laboratory by passages in infected mice were used for the determination. *Cryptosporidium* oocysts were purified from the feces from the mice by a combination of discontinuous density sucrose gradient centrifugation and cesium chloride gradient centrifugation and enumerated with a hemacytometer. The RNA of purified and enumerated oocysts was extracted, and used as template RNA. The template RNA was prepared in 10-fold serial dilutions. Then cDNA was synthesized through reverse transcription. Next, the real-time PCR assay was performed in triplicate for each diluted cDNA solution using chemically synthesized oligo-DNA as standard DNA.

3.8. Microscopic observation

The conventional microscopic observation was performed by Japanese standard method for detection of *Cryptosporidium* oocysts in water supply systems (Ministry of Health, Labor and Welfare, 2007). After purification through immunomagnetic separation, *Cryptosporidium* oocysts were fixed on a membrane filter. The fixed sample was stained with Easy-Stain antibody stain (BTF, North Ryde, Australia), and

observed using an epifluorescent microscope (IX71; Olympus, Tokyo, Japan).

4. Results and discussion

4.1. Standard curve of ABC-PCR assay

We constructed a standard curve for the quantification of the 18S rRNA of *Cryptosporidium* spp. Various amounts of the DNA fragment encoding the partial 18S rRNA genes of *C. hominis* as target standard DNA, ranging from 10^1 to 10^5 copies in the presence of 10^3 copies of competitor DNA, were prepared. The DNA mixtures were amplified by PCR followed by measuring the fluorescence of the DNA mixtures. $[(G_{60}/G_{95}) - G_U]/[R_U - (R_{60}/R_{95})]$ values were plotted against the starting quantity of the target DNA (Fig. 2). The results show that $[(G_{60}/G_{95}) - G_U]/[R_U - (R_{60}/R_{95})]$ values obtained from triplicate samples closely match a rectangular hyperbola with a correlation coefficient (R) of 0.9997. The standard deviation (SD) of triplicate determinations was less than 0.008 for 10^1 to 10^5 copies. These results indicate that the ABC-PCR assay was quantitative and reproducible for the measurement of the number of copies of 18S rRNA of *Cryptosporidium* spp. Although the quantification range of the ABC-PCR assay is narrower than that of the real-time PCR assay, we can adjust the range by varying the addition quantity of internal standard DNA according to sample concentration, as written in our previous paper (Miyata et al., 2010).

4.2. The number of 18S rRNA molecules in a Cryptosporidium oocyst

Fig. 3 shows the relationship between the number of *Cryptosporidium* oocysts and the number of copies of 18S rRNA molecules of *C. parvum* as determined by the real-time RT-PCR assay. The ratio of the oocyst number to copy number was independent of the initial concentration of template RNA because reverse transcription and cDNA amplification proceeded effectively under this experimental condition. It was found that one standard *Cryptosporidium* oocyst has approximately 32,700 copies of 18S rRNA molecules. This value was used for the calculation (conversion) of the number of *Cryptosporidium* oocysts from the number of gene copies in water samples as determined by the ABC-RT-PCR and real-time RT-PCR assays although this conversion ratio may vary a little depending on the activity of *Cryptosporidium* oocysts.

Meanwhile, it has been reported that each *Cryptosporidium* genome in one oocyst has 20 copies of 18S rRNA genes (Abrahamsen et al., 2004). Therefore, it is possible to detect *Cryptosporidium* oocysts without reverse transcription. However, the number of copies of rRNA genes is much lower than that of rRNA molecules. If we try to quantify *Cryptosporidium* oocysts without reverse transcription, labor-intensive high condensation of water samples may be needed. In addition, duplicate or triplicate examination is almost impossible if there is only one *Cryptosporidium* oocyst in the water sample. Hence, we added reverse transcription process to increase the sensitivity.

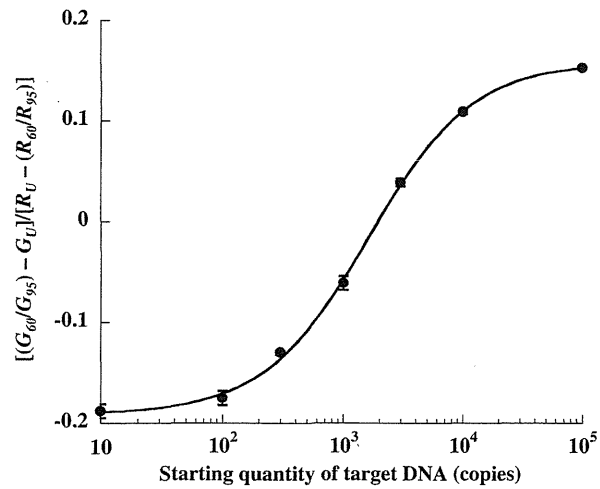

Fig. 2 – Typical standard curve. A fixed amount of the internal standard (10^3 copies) was coamplified with various amounts of the target standard DNA in triplicate. The standard curve was obtained by fitting the data points to a rectangular hyperbola. $y = -559.8/(x + 1602) + 0.1583$, and the correlation coefficient (R) was calculated to be 0.9997. The error bars represent the standard deviation (SD) of triplicate determinations per dilution.

4.3. Quantification of Cryptosporidium oocysts in water samples by ABC-RT-PCR assay

The number of copies of the 18S rRNA molecules of *Cryptosporidium* spp. naturally present in 14 water samples were quantified using ABC-RT-PCR and real-time RT-PCR. Then the copy number was converted to the number of *Cryptosporidium* oocysts using a conversion coefficient determined by the above mentioned experiment. As shown in Table 2 and Fig. 4, concentrations of *Cryptosporidium* oocysts in river water samples were successfully quantified by the ABC-RT-PCR assay. The quantified values by the ABC-RT-PCR assay are very closely resembling those by the real-time RT-PCR assay.

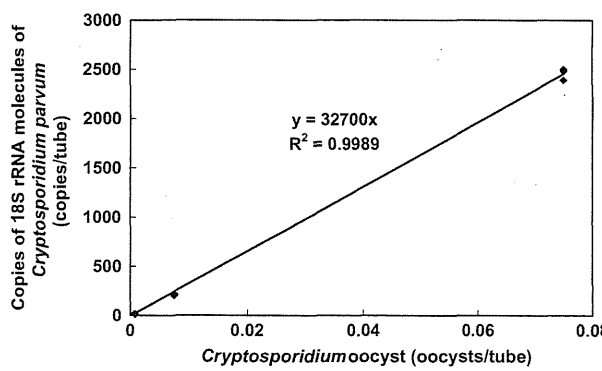

Fig. 3 – Relationship between the number of *Cryptosporidium* oocysts and the number of copies of 18S rRNA molecules of *Cryptosporidium* spp. as determined by real-time RT-PCR.

Table 2 – Three methods of quantifying *Cryptosporidium* oocysts in surface water samples.

Sample	ABC-PCR (oocysts/10 L)	Real-time PCR (oocysts/10 L)	Microscopic observation (oocysts/10 L)
A	0.23	0.33	2
B	6.6	7.3	–
C	0.076	–	2
D	6.6	11	4
E	–	–	–
F	–	–	–
G	0.67	1.4	4
H	38	30	12
I	0.13	0.17	0
J	19	26	14
K	0.57	0.036	10
L	38	30	30
M	0.98	0.36	16
N	49	71	40

The coefficient of determination (R^2) value at the linear least squares method between the two PCR assays was 0.89. In addition, the quantified concentration in most water samples by PCR assays was comparable to that by conventional microscopic observation although the principle of quantification is different, and the conversion ratio of the number of copies of 18S rRNA molecules to that of *Cryptosporidium* oocysts may vary a little depending on the activity of *Cryptosporidium* oocysts in river water samples. Therefore, it is considered that *Cryptosporidium* oocysts can be specifically determined by the ABC-RT-PCR assay. In addition, the fluorescence intensity of red dye at the end-point of PCR was significantly decreased in all samples (data not shown), which indicates false-negative results were not obtained in this study. Thus, *Cryptosporidium* oocysts in real water samples can be simply and accurately quantified using the ABC-RT-PCR assay. As the only equipment that is needed for this end-point fluorescence assay is a simple fluorometer and a relatively inexpensive thermal cycler, this method can markedly reduce time and cost to quantify *Cryptosporidium* oocysts. Moreover, this method can be easily applied to quantify many other health-related water microorganisms because it is very easy to design primers and ABProbes. If primers and probes of the real-time (TaqMan) PCR assay are published, in the ABC-PCR assay, the same primers can be used. The only thing that the users need to do is to modify the sequence of ABProbe a little bit from the TaqMan probe in the same manner in this study.

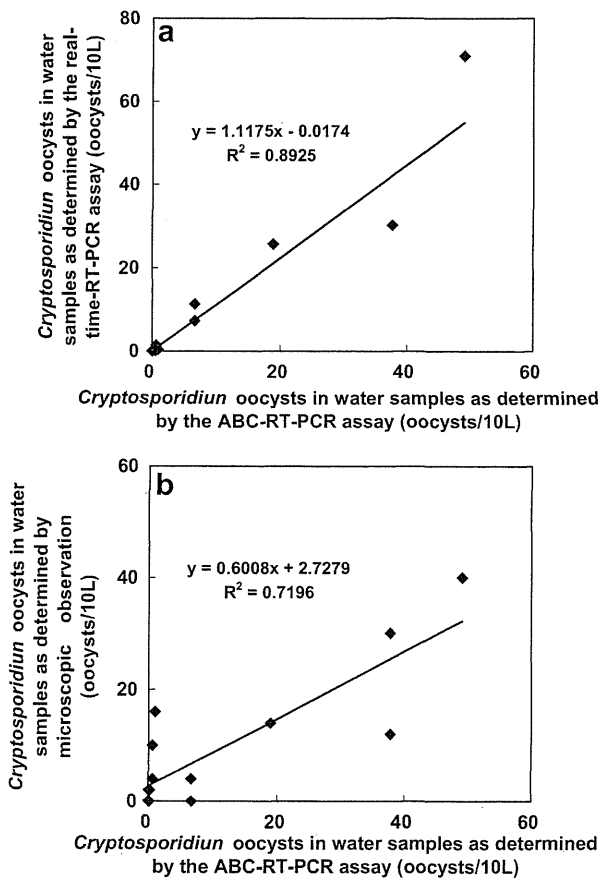

Fig. 4 – Relationship between the number of *Cryptosporidium* oocysts in water samples as determined by (a) ABC-RT-PCR and real-time RT-PCR (b) ABC-RT-PCR and microscopic observation.

Meanwhile, a few data (Sample K and M in Table 2) quantified by two PCR assays were much smaller than those by microscopic observation. It is well known that environmental samples contain PCR inhibitors such as humic acids, and the number of target DNA is underestimated by quantitative PCR assays due to the existence of inhibitors. However, in the ABC-PCR assay, accurate quantification is attained regardless of the existence of PCR inhibitors because internal standard DNA is used, and the effect of PCR inhibition on quantification is canceled (Tani et al., 2007). In addition, sample purification using immunomagnetic separation was carefully performed. Therefore, PCR inhibition must not be the main reason for the underestimate. Another suspected reason is that not all *Cryptosporidium* oocysts in river water samples contain the same amount of the 18S rRNA molecules. Although it has been reported that the 18S rRNA molecules of *Cryptosporidium* oocysts are more stable than mRNA molecules like β-tubulin (Widmer et al., 1999); reportedly, the number of copies of 18S rRNA molecules in *Cryptosporidium* oocysts significantly decreased when those were inactivated by heat shock (95 °C

for 4 h) (Fontaine and Guillot, 2003), which indicates that the number of copies of 18S rRNA molecules would reflect the viability of *Cryptosporidium* oocysts. Therefore, if dead or damaged *Cryptosporidium* oocysts existed in river water samples, both the number of copies of 18S rRNA molecules and the converted values of *Cryptosporidium* oocysts as determined by two RT-PCR assays would be small. It was reported that there were many dead (non-viable) *Cryptosporidium* oocysts in the effluent discharged from many swine wastewater treatment facilities that were one of the main pollution sources in river water (Jenkins et al., 2010), which indicates that dead *Cryptosporidium* oocysts exist in river water depending on the place and time. Hence, a few data (Sample K and M in Table 2) quantified by two RT-PCR assays would be much lower than those by microscopic observation.

5. Conclusion

In this study, we developed an ABC-RT-PCR assay for simple and cost-effective quantification of *Cryptosporidium* oocysts in water samples. The following are the main outcomes of this study.

(1) The standard curve of the ABC-PCR targeting 18S rRNA of *Cryptosporidium* spp. had a good fitting to a rectangular hyperbola with high correlation coefficient, and standard deviation of triplicate determinations was low. The ABC-PCR assay was quantitative and reproducible for the measurement of number of copies of 18S rRNA genes of *Cryptosporidium* spp.
(2) Concentrations of *Cryptosporidium* oocysts in river water samples were successfully quantified by the developed ABC-RT-PCR assay. The quantified values by the ABC-RT-PCR assay very closely resembled those by the real-time RT-PCR assay.
(3) Most quantified values by the ABC-RT-PCR assay were comparable to those by microscopic observation. However, a few values quantified by the ABC-RT-PCR assay were much smaller than those by microscopic observation, which indicates that dead or damaged *Cryptosporidium* oocysts, which have only a small number of copies of 18S rRNA molecules, exist in river water depending on the place and time. In this case, the sensitivity of the ABC-RT-PCR assay would be lower than that by microscopic observation.
(4) As the only equipment that is needed for the ABC-RT-PCR assay is a simple fluorometer and a relatively inexpensive thermal cycler, this method can markedly reduce time and cost to quantify *Cryptosporidium* oocysts in water samples.

Acknowledgments

This study was financially supported by a Grant-in-Aid for Research Activity Start-up (21860094), Japan Society for the Promotion of Science (JSPS).

REFERENCES

Abrahamsen, M.S., Templeton, T.J., Enomoto, S., Abrahante, J.E., Zhu, G., Lancto, C.A., Deng, M., Liu, C., Widmer, G., Tzipori, S., Buck, G.A., Xu, P., Bankier, A.T., Dear, P.H., Konfortov, B.A., Spriggs, H.F., Iyer, L., Anantharaman, V., Aravind, L., Kapur, V., 2004. Complete genome sequence of the apicomplexan, *Cryptosporidium parvum*. Science 304 (5669), 441–445.

Altschul, S.F., Gish, W., Miller, W., Myers, E.W., Lipman, D.J., 1990. Basic local alignment search tool. Journal of Molecular Biology 215 (3), 403–410.

Carpenter, C., Fayer, R., Trout, J., Beach, M.J., 1999. Chlorine disinfection of recreational water for *Cryptosporidium parvum*. Emerging Infectious Diseases 5 (4), 579–584.

Fontaine, M., Guillot, E., 2003. Study of 18S rRNA and rDNA stability by real-time RT-PCR in heat-inactivated *Cryptosporidium parvum* oocysts. FEMS Microbiology Letters 226 (2), 237–243.

Garcés-Sanchez, G., Wilderer, P.A., Munch, J.C., Horn, H., Lebuhn, M., 2009. Evaluation of two methods for quantification of *hsp70* mRNA from the waterborne pathogen *Cryptosporidium parvum* by reverse transcription real-time PCR in environmental samples. Water Research 43 (10), 2669–2678.

Jenkins, M.B., Liotta, J.L., Lucio-Forster, A., Bowman, D.D., 2010. Concentrations, viability, and distribution of *Cryptosporidium* genotypes in lagoons of swine facilities in the Southern Piedmont and in coastal plain watersheds of Georgia. Applied and Environmental Microbiology 76 (17), 5757–5763.

Keegan, A.R., Fanok, S., Monis, P.T., Saint, C.P., 2003. Cell culture-Taqman PCR assay for evaluation of *Cryptosporidium parvum* disinfection. Applied and Environmental Microbiology 69 (5), 2505–2511.

King, B.J., Keegan, A.R., Monis, P.T., Saint, C.P., 2005. Environmental temperature controls *Cryptosporidium* oocyst metabolic rate and associated retention of infectivity. Applied and Environmental Microbiology 71 (7), 3848–3857.

Kurata, S., Kanagawa, T., Yamada, K., Torimura, M., Yokomaku, T., Kamagata, Y., Kurane, R., 2001. Fluorescent quenching-based quantitative detection of specific DNA/RNA using a BODIPY((R)) FL-labeled probe or primer. Nucleic Acids Research 29 (6), e34.

Miller, W.A., Gardner, I.A., Atwill, E.R., Leutenegger, C.M., Miller, M.A., Hedrick, R.P., Melli, A.C., Barnes, N.M., Conrad, P. A., 2006. Evaluation of methods for improved detection of *Cryptosporidium* spp. in mussels (*Mytilus californianus*). Journal of Microbiological Methods 65 (3), 367–379.

Ministry of Health, Labor and Welfare, Japan, 2007. Methods for the Detection of *Cryptosporidium* Oocysts, *Giardia* Cysts and Indicator Microorganisms in Water Supply Systems Tokyo, Japan (in Japanese).

Miyata, R., Adachi, K., Tani, H., Kurata, S., Nakamura, K., Tsuneda, S., Sekiguchi, Y., Noda, N., 2010. Quantitative detection of chloroethene-reductive bacteria *Dehalococcoides spp.* using alternately binding probe competitive Polymerase Chain Reaction. Molecular and Cellular Probes 24 (3), 131–137.

Nichols, G., 2008. Epidemiology. In: Fayer, R., Xiao, L. (Eds.), Cryptosporidium and Cryptosporidiosis, second ed. IWA Publishing, London, UK, pp. 79–118.

Noda, N., Tani, H., Morita, N., Kurata, S., Nakamura, K., Kanagawa, T., Tsuneda, S., Sekiguchi, Y., 2008. Estimation of single-nucleotide polymorphism allele frequency by alternately binding probe competitive polymerase chain reaction. Analytica Chimica Acta 608 (2), 211–216.

Oda, T., Ito, H., Yano, H., Rai, S.K., Kawabata, M., Inoue, M., Uga, S., 2002. Use of hydrophilic polytetrafluoroethylene (HPTFE) membrane in detecting *Cryptosporidium* oocysts from source

water. Japanese Journal of Water Treatment Biology 38 (3), 153–158.
O'Donoghue, P.J., 1995. *Cryptosporidium* and cryptosporidiosis in man and animals. International Journal of Parasitology 25 (2), 139–195.
Peeters, J.E., Mazás, E.A., Masschelein, W.J., Villacorta Martiez de Maturana, I., Debacker, E., 1989. Effect of disinfection of drinking water with ozone or chlorine dioxide on survival of *Cryptosporidium parvum* oocysts. Applied and Environmental Microbiology 55 (6), 1519–1522.
Ramirez, N.E., Sreevatsan, S., 2006. Development of a sensitive detection system for *Cryptosporidium* in environmental samples. Veterinary Parasitology 136 (3–4), 201–213.
Tani, H., Kanagawa, T., Kurata, S., Teramura, T., Nakamura, K., Tsuneda, S., Noda, N., 2007. Quantitative method for specific nucleic acid sequences using competitive polymerase chain reaction with an alternately binding probe. Analytical Chemistry 79 (3), 974–979.
Torimura, M., Kurata, S., Yamada, K., Yokomaku, T., Kamagata, Y., Kanagawa, T., Kurane, R., 2001. Fluorescence-quenching phenomenon by photoinduced electron transfer between a fluorescent dye and a nucleotide base. Analytical Science 17 (1), 155–160.
Widmer, G., Orbacz, E.A., Tzipori, S., 1999. β-tubulin mRNA as a marker of *Cryptosporidium parvum* oocyst viability. Applied and Environmental Microbiology 65 (4), 1584–1588.
Yagita, K., Izumiyama, S., Tachibana, H., Masuda, G., Iseki, M., Furuya, K., Kameoka, Y., Kuroki, T., Itagaki, T., Endo, T., 2001. Molecular characterization of *Cryptosporidium* isolates obtained from human and bovine infections in Japan. Parasitology Research 87 (11), 950–955.

AEM
Journals.ASM.org

Depletion of *Cryptosporidium parvum* Oocysts from Contaminated Sewage by Using Freshwater Benthic Pearl Clams (*Hyriopsis schlegeli*)

Toshihiko Izumi,[a] Kenji Yagita,[b] Shinji Izumiyama,[b] Takuro Endo,[b] and Yasoo Itoh[a]

Section of Drinking Water Chemistry, Division of Environmental Hygiene, Hokkaido Institute of Public Health, Sapporo, Japan,[a] and Protozoa Laboratory, Department of Parasitology, National Institute of Infectious Diseases, Toyama, Tokyo, Japan[b]

The freshwater benthic pearl clam, *Hyriopsis schlegeli*, was experimentally exposed to *Cryptosporidium parvum* oocysts, and it was verified that the oocysts were eliminated predominantly via the fecal route, retaining their ability to infect cultured cells (HCT-8). The total fecal oocyst elimination rate was more than 90% within 5 days after exposure to the oocysts. *H. schlegeli* was able to survive in the final settling pond of a sewage plant for long periods, as confirmed by its pearl production. In the light of these findings, the clam was placed in the final settling pond in a trial to test its long-term efficacy in depleting oocysts contaminating the pond water. The number of clams placed was set to ensure a theoretical oocyst removal rate of around 50%, and the turbidity and the density of feed microbes in the overflow trough water of the pond were about 35% and 40 to 60% lower, respectively, than in the control water throughout the year. It was found that the clam feces containing oocysts were sufficiently heavy for them to settle to the bottom of the pond, despite the upward water flow. From these results, we concluded that efficient depletion of oocysts in the sewage water of small or midscale sewage treatment plants can be achieved by appropriate placement of *H. schlegeli* clams.

A large number of studies have investigated the presence of *Cryptosporidium* oocysts in clams, and biomonitoring of this protozoan has been attempted in field tests with various clam species (3, 5, 6, 9–15, 17, 26–30, 34, 41, 43). There have also been many basic research studies on the biological functions of clams (1, 2, 7, 17, 21, 22, 25, 31–33, 36, 37, 39, 40, 49, 51, 52). However, the issue of accumulation and/or filtration of *Cryptosporidium* oocysts from water has received little attention, perhaps because of the difficulties in maintaining clams for long periods under artificial conditions in the laboratory. We have already established that *Corbicula japonica*, a brackish water benthic clam, might be applicable for removal of *Cryptosporidium* oocysts from contaminated river water (23, 24). Here, we report a study in which we attempted to develop an aquatic biological filtration system that could be practically applied for depletion of oocysts from contaminated water. Our study utilized a large Japanese freshwater benthic clam, *Hyriopsis schlegeli*, which has a water filtration capacity potentially superior to that of *C. japonica*. *H. schlegeli* belongs to the Unionidae and is the largest native freshwater pearl clam with a long life span. It was originally endemic to the area around Lake Biwa, Shiga, Japan, and has since been widely transplanted around Japan as a pearl clam. It is a gonochorismal, oviparous clam with a unique reproductive ecology: its larvae, known as glochidia, hatch on the gills of the clam and are released from the exhalant siphon. They then develop benthically after some weeks of parasitic life on the epidermis of fish. *H. schlegeli* was used effectively in the present study because of the ease with which its reproduction can be controlled, owing to its unique ecology, long life span, and the well-established nursery techniques that have been developed for it as a pearl clam. However, there have been very few previous reports on the basic biological potential and functions of freshwater clams, including *H. schlegeli*, under laboratory conditions. Before conducting long-term trials of this clam in a sewage treatment plant, it was necessary to examine its biological potential, including its water filtration rates and other parameters, in the laboratory. This is because there has been a lack of fundamental ecological data on *H. schlegeli*, such as its choice of food, the appropriate amount of food to supply, how to supply it, and the optimum laboratory cistern conditions for ensuring low clam mortality, without the clam ejecting pseudofeces or lapsing into a fasting state (23, 24). Based on the data obtained in preliminary tests, long-term trials were carried out to evaluate the efficacy of oocyst removal from water when using *H. schlegeli* clams as a biological filter in the final settling pond of a sewage treatment plant.

This first report details the basic potential of *H. schlegeli* clams maintained under artificial laboratory conditions and provides valuable data for the application of the clams to depletion of *Cryptosporidium* oocysts in the final settling pond of a sewage plant.

MATERIALS AND METHODS

Preliminary investigations of *H. schlegeli*. (i) Facilities for housing *H. schlegeli*. *H. schlegeli* clams with body weights of 50 to 500 g, including the shells, were purchased from the Yanase Pearl Company, Ltd., Ibaraki, Japan. The unit for housing the clams comprised a styrene foam outer cistern (15 liters) for temperature retention and a resinous inner cistern (8 liters) as an environment for the clams (see Fig. S1 in the supplemental material). The outer cistern was filled with tap water and contained a stirring magnet, a water temperature sensor, and the cooling pipe of a cooling unit (RZ-90; REI-SEA, Japan), and the whole arrangement was set on a magnetic stirrer. The inner cistern contained dechlorinated tap water, a stirring magnet, and a pumice stone for aeration and circulation. The water in the outer cistern was usually kept at 20°C, and the clams were oriented horizontally in a multistory stainless steel cage placed in the inner

Received 13 May 2012 Accepted 6 August 2012
Published ahead of print 17 August 2012
Address correspondence to Toshihiko Izumi, izumit@iph.pref.hokkaido.jp.
Supplemental material for this article may be found at http://aem.asm.org/.

doi:10.1128/AEM.01502-12

cistern. All of the water in the inner cistern was changed once a day, as no water filtration apparatus was installed.

(ii) Feeding. Powder-type chow (BV-01; DIC-Lifetech, Japan) consisting of *Spirulina* (*Arthrospira platensis*) for the Japanese short-necked clam (*Ruditapes philippinarum*) mixed with about 5% powdered chlorella (*Chlorella pyrenoidosa*; Sun Chlorella, Japan) was used as chow. Chow equivalent to 0.2 to 0.3% of the total clam body weight was suspended in a small volume of water, and following 5 min of ultrasonic treatment to ensure uniform distribution this was supplied to the clams in the inner cistern, six times a day at 2-h intervals during the daytime (total chow volume, 1.2 to 1.8% of the clam total body weight/day). Liquid chow (Micro-Vert, Kent Marine) for invertebrates and "green water," consisting of phytoplankton cultivated in a tank with appropriate amounts of chemical fertilizer, under adequate sunlight and aeration, were added several times a week as supplementary chow.

(iii) Nitrogen-oxidizing bacteria. To oxidize and detoxify the ammonia and nitrites generated by the clam excreta, which are toxic to the clam, 0.3 ml/liter of nitrogen-oxidizing bacteria (Power Bacter PG; Ecological Laboratories Inc.) was added to the water in the inner cistern after every water change.

To estimate the suitability of the laboratory conditions for maintaining *H. schlegeli* clams, the mortality [as a percentage; 100 × (number of dead clams/number of total clams)] during 3 years (from July 2007 to June 2010) was calculated using 60 clams (50 to 70 g) kept under the conditions described above.

Balance study using *C. parvum* oocysts with *H. schlegeli* clams. To understand the internal accumulation of *C. parvum* oocysts in the clams and the pattern of oocyst excretion from the clam body after exposure to oocysts, an internal oocyst distribution and excretion study (balance study) was carried out as follows.

C. parvum oocysts (H8 strain) were provided by the Protozoa Laboratory, Department of Parasitology, National Institute of Infectious Diseases, Tokyo, Japan, and stored at 4°C (50). A total of 24 *H. schlegeli* clams (50 to 70 g) were used in groups of three. After 6 weeks of acclimation at 20°C, three randomly selected control clams were removed from the inner cistern to confirm the absence of any nonendogenous protozoans in them. After 12-h starvation of the clams to collect fresh feces, 1.99×10^6 oocysts (2.49×10^5 oocysts/liter; 9.48×10^4 oocysts/clam), within 3 weeks after preparation from mouse feces, were added to the inner cistern housing the remaining clams. After addition of the oocysts, three randomly selected *H. schlegeli* clams were sacrificed at 24-h intervals for 7 days.

The water in the inner cistern was sampled, and the clam feces were collected daily. The gastrointestinal (GI) tract, gills, and mantle excised from the removed clams were ground in a mixer (IKA Labor Technik, Switzerland) with a buffer (B100-20; Waterborne, Inc.), followed by oocyst separation with a magnetic bead kit (GC-Combo; Dynabeads). After preheating treatment (100°C, 5 min) to increase stainability with DAPI (4′,6-diamidino-2-phenylindole dihydrochloride; Sigma, St. Louis, MO) (20), the oocysts were applied to a 4-well glass slide (C.A. Hendley Ltd., United Kingdom) and then stained using a direct immunofluorescence assay kit (Aqua-Glo G/C Direct FL; Waterborne, Inc.) in an incubator at 37°C, followed by DAPI treatment for nuclear staining. The oocysts, stained with fluorescent reagents, were dried at 42°C in a drying oven, followed by methanol fixation. DABCO (1,4-diazabicyclo-2,2,2-octane; Sigma)-glycerin (1:63) was then added dropwise, and a coverglass was placed on the wells, which were then sealed with nail enamel. Identification and enumeration of *C. parvum* oocysts were carried out with a fluorescence microscope (DM LB2; Leica, Germany) under the conditions described elsewhere (23).

The feces were collected by centrifugation (3,000 rpm, 10 min) and treated three times with acetone to remove the high-viscosity component, followed by application to a direct immunofluorescence assay kit and DAPI staining as described above. The cistern water was processed using a mixed cellulose ester membrane filter (A100A090C; Advantec, Japan) dissolution method, followed by treatment with acetone removal of contaminants on a Percoll (Pharmacia Biotech)-sucrose density gradient and staining with fluorescence dyes in a manner similar to that described above (23).

DNA extraction and PCR. Together with the balance study described above, we conducted PCR on the *H. schlegeli* clams exposed to *C. parvum* oocysts to screen for the presence of oocysts based on detection of *C. parvum* DNA. Feces and GI tract samples from the clams were collected at 1, 3, and 5 days after exposure to the oocysts and examined for *C. parvum* DNA by PCR using the TRAP-C2-F and TRAP-C2-R primer pair, corresponding to positions 848 to 867 on the coding strand and 1180 to 1199 on the negative strand of GenBank sequence X77586, as reported elsewhere (23), while an internal control (IC; 542 bp), to ensure sufficient progress of the PCR, was applied to only the negative control. The IC was prepared from the PCR product (369 bp), the BssHII-digested fragment, and the Klenow-blunted multiple cloning site from pBluescript KS$^-$ by using a rapid DNA ligation kit (Roche, Switzerland) (23).

***In vitro* infection test for fecal *C. parvum oocysts* using cultured cells.** In order to determine whether *C. parvum* oocysts are digested by *H. schlegeli* clams, or whether they remain infectious after ingestion *in vitro*, qualitative detection of *C. parvum* oocysts obtained from clam feces was carried out using cultured human colon tumor (HCT-8) cells, as reported elsewhere (19, 45, 48) and described briefly below.

Feces collected from clams exposed to *C. parvum* oocysts at a rate of 9.48×10^4 oocysts/clam and pooled in phosphate-buffered saline were prepared for purification of the oocysts in a sucrose density gradient. The purified oocysts were then processed with acid followed by treatment with trypsin (Difco) for 2 h and then subjected to *in vitro* cell culture for detection of infectiousness during 7 days. Meronts in the HCT-8 cells were stained with an immunofluorescent agent (Sporo-Glo; Waterborne, Inc.) and observed using a fluorescence microscope at 200× magnification. A detailed assessment of HCT-8 cell infection with oocysts was then conducted by counting the number of foci per visual field on the culture plate.

Water and oocyst filtration abilities of *H. schlegeli* clams. To determine the water filtration and oocyst filtration capacities of *H. schlegeli*, a multistory stainless steel cage containing two clams (each weighing 500 g) was set in the inner cistern, and a trial was carried out using 6.6×10^5 *C. parvum* oocysts/liter (1.7×10^6 oocysts/clam) and 28 mg/liter feed at 20°C. After the start of the trial, water samples (10 ml) were collected every 15 min for 60 min, and the turbidity, expressed in nephelometric turbidity units (NTU), was measured with a water analyzer (Water Analyzer-2000; Nippon, Denshoku Kogyo, Japan). The water samples were also set in a hemacytometer, and the number of oocysts was counted under a microscope at ×200. A similar experiment was conducted without feed as a control. To ascertain whether *H. schlegeli* clams were able to filter and ingest the oocysts in water of the final settling pond water, a test of oocyst filtration by clams was carried out using water from the final settling pond containing microbes and oocysts at 6.6×10^5 *C. parvum* oocysts/liter (1.7×10^6 oocysts/clam) in a manner similar to that described above (see also Fig. S2 and S3 in the supplemental material).

In addition, the following experiments were carried out at three water temperatures (15, 20, and 25°C) using each of seven concentrations (9, 14, 28, 42, 84, 168, and 336 mg/liter) of powder-type chow together with 6.6×10^5 *C. parvum* oocysts/liter (1.7×10^6 oocysts/clam). The water turbidity was determined and plotted versus time, and the linear coefficient and the value of the y intercept of the linear function ($y = ax + b$, where y is the turbidity, x is time, a is the linear coefficient, and b is the y intercept value) were calculated. The time (x_0) to zero turbidity was calculated by extrapolating the linear function obtained, and the water filtration rate (in liters/h) per clam was calculated using the following formula: (cistern water volume)/[(x_0)(number of clams)].

Field survey of the sewage plant using *H. schlegeli* clams. For the effective removal of *Cryptosporidium* oocysts from contaminated water by addition of *H. schlegeli* clams, the following field surveys were carried out with the clams in the final settling pond of the Sosei River wastewater treatment plant, Sapporo, Japan.

Confirmation of water quality in the final settling pond by cultivation of fish and pearls and chemical analysis. Tests of the biological suitability of the pond water for survival of *H. schlegeli* clams were carried out by cultivation of fish and pearls in the pond and by chemical water analysis of the water.

We utilized ubiquitous freshwater fish that wide inhabiting the same water systems as *H. schlegeli* clams in Japan, the slender bitterling (*Tanakia lanceolata*), known to lay eggs in Unionidae clams, and the silver crucian carp (*Carassius gibelio langsdorfi*), known to be the most common fish in the lower reaches and ponds in Japan. Fish were kept for 2 weeks in 1-liter glass beakers filled with water from the final settling pond at room temperature. The water in the beakers was exchanged daily, and the suitability of the water for rearing of the clams was determined by observing the behaviors of the fish, including any evident breathing difficulty, changes of body color, and feeding status (fasting).

After these observations, a further test to verify the suitability of the pond water for long-term survival of the clams in the water of the final settling pond was conducted by observing pearl production by *H. schlegeli* clams over a 3-year period (from September 2007 to October 2010). Twelve clams (500 g), with pearl cores inserted, were placed horizontally in two nylon net holders (40-cm width by 60-cm length), each with six compartments of 20 by 20 cm, with one clam per compartment. The nets were placed horizontally at a vertical interval of 20 cm in a specially made 2-story stainless steel cage (40-cm width by 60-cm length) covered with a resin-treated dust-proof double-folded agricultural polyester sunscreen net (mesh size, 1 mm; Toyobo, Japan) at the sides. This cage was set along the wall of the overflow trough in the final settling pond at a water depth of 15 to 35 cm. After 3 years, the quality of the pond water for survival of the clam was estimated in terms of both clam mortality and clam pearl production, as the latter would clearly reflect the long-term water quality.

To conduct chemical analysis of the water in the final settling pond, the pond water was analyzed monthly for more than 2 years, from August 2006 to December 2008, prior to and during the trial with the *H. schlegeli* clams described immediately above. The basic analytical procedures used for metals (Al, Ba, Ca, Cd, Cr, Cu, Fe, Mg, Mn, Pb, and Zn) and determination of nitrogen (N) from ammonia and nitrites in the water have been described elsewhere (23). Determination of total phosphorus (TP) and phosphorus derived from soluble phosphate ions ($P\text{-}PO_4^{3-}$) in the water was conducted using the ascorbic acid method (16). Dissolved oxygen (DO) at a water depth of 50 cm was measured by the azide modification method (16), electrical conductivity (EC) was determined with a conductivity meter (ES-51; Horiba Ltd., Japan), and pH was measured with a D-52 pH meter (Horiba Ltd., Japan).

Measurement of water volume passing through the final settling pond and placement of *H. schlegeli* clams in the pond. The final settling pond for separating sediment from the pretreated sewage (see Fig. S2 in the supplemental material) measured 4.3 m (width) by 32.2 m (length) by 2.0 m (depth) and had two overflow troughs (0.5-m width by 20.0-m length by 0.3-m depth) along the sides. After biological treatment of the sewage by using the activated sludge, the treated water was introduced into the pond, and any sediment in the water settled there. The overflow entered the overflow troughs, and from there it was chlorinated for disinfection and then released into a river. Meanwhile, the precipitated sediment was gathered with caterpillar-type spatulas set in the bottom of the pond. The residue evacuated from the pond was then disinfected by automated heat treatment.

The overflow water volume (in L/h) of the pond was calculated from the total drained water volume and the surface area of the pond.

The clams were placed in the final settling pond of the sewage plant because the water further downstream of the final settling pond is disinfected with sodium hypochlorite at around 2.0 mg/liter, which would make it impossible for clams to survive.

The clams were arranged to provide a practical filter of the overflow water. Twenty-four clams (total body weight, 500 g) were placed horizontally in two nylon net holders, each with six compartments, two clams per compartment, in the same manner as that described for clam pearl production, thus creating a substantial density of 1 clam per 100 cm^2. Fourteen cages with a total of 168 clams were placed two deep, along the overflow trough at a water depth of 15 to 35 cm, covering overall about 40% of the water surface area along the overflow trough. Fourteen cages without clams were set in the same manner along the side of the opposite overflow trough of the settling pond as a control. (See Fig. S3 in the supplemental material.)

After placing the clams in the final settling pond, any suspended dirt adhering to the nets around the cages was washed off once a week by spraying with water.

Fecal precipitation of *H. schlegeli* clams in the final settling pond. Measurements of the rate of fecal precipitation by *H. schlegeli* clams were conducted to establish whether clam excreta would precipitate to the bottom of the final settling pond, where there is a constant slow upward water flow from the lower to the higher water layers. This test ensured that feces containing *Cryptosporidium* oocysts would precipitate to the bottom of the settling pond, where heat treatment could be carried out.

The test was conducted in the laboratory, and to simulate the upward water flow, a desiccator (25-cm diameter, 25-cm height) with a soft resinous tube muzzle introducing tap water at the bottom of the vessel was used. The muzzle of the tube was set to point upward in the center at the bottom of the desiccator to generate the upward water flow. The rate of upward flow was set at 2.0 cm/s, as the corresponding rate in the final settling pond was lower than this, and the flow was measured by a current meter (Hiroi type; Rigou, Japan). Measurements of the rate of fecal precipitation by *H. schlegeli* clams were carried out by dropping mucous feces from the clams in the center of the surface of the desiccator and observing their precipitation.

Estimation of removal of *C. parvum* oocysts from water by *H. schlegeli* clams in the final settling pond. To estimate of the efficacy of oocyst removal by the clams in the pond, changes in turbidity and microbe density in the overflow trough water were determined.

As protozoa, such as *Cryptosporidium*, were not always detected in the final settling pond, we used substitute parameters for *Cryptosporidium* oocysts in order to estimate oocyst removal by the clams: the reduction of water turbidity and the reduction in concentrations of the specific microbes *Heterochromulina* sp., *Gymnamoebia* sp., *Testacealobosia* sp., and *Vorticella* sp.

A 1-year experiment, conducted from October 2007 to December 2008, measured these parameters monthly to verify the ability of the clam to remove *Cryptosporidium* oocysts in the final settling pond. Overflow trough water from the region of the cages was collected and examined. The turbidity was measured using a water analyzer as described above, and the turbidity removal rate (as a percentage) was calculated as follows: $100 \times [1 - (\text{turbidity with the clams})/(\text{turbidity without the clams})]$. On the other hand, the density of microorganisms was measured by adding of 2.0 ml of Lugol's iodine solution to 1,000 ml of the overflow trough water and allowing it to settle overnight at room temperature to precipitate the microorganisms. The supernatant was then drained to a final volume of 20 ml by aspiration, and this water sample was added dropwise to the blood counting chamber of a hemacytometer, followed by microscopic observations at 400× magnification to count phytoplankton and zooplankton. Meanwhile, the microbe removal rate (as a percentage) was calculated as follows: $100 \times [1 - (\text{microbe density with the clams})/(\text{microbe density without the clams})]$.

RESULTS

Preliminary investigations using *H. schlegeli* clams. Only two dead *H. schlegeli* clams were noted in the laboratory cistern during the 3-year period, and the clam mortality rate was calculated to be 3.3%. In view of this low mortality, it was considered that there would be no particular problem in maintaining clams in the laboratory.

The results of the balance study of the *C. parvum* oocysts de-

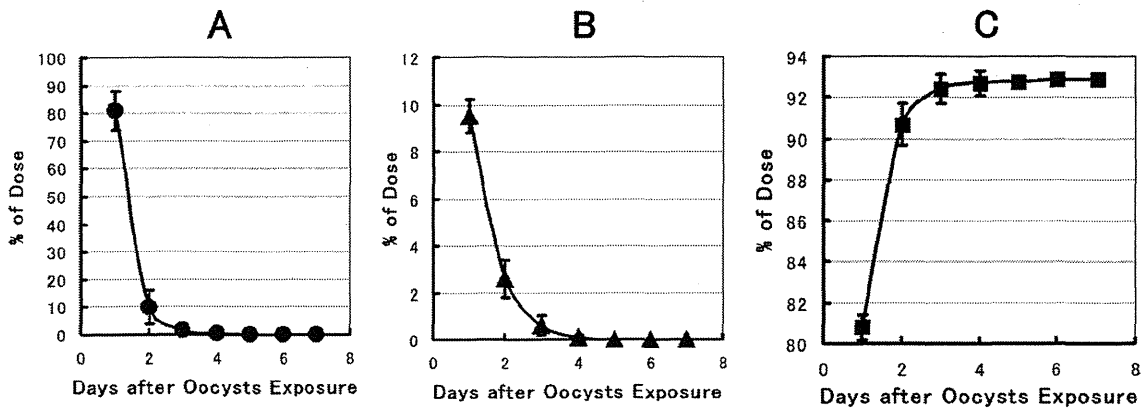

FIG 1 Relative amounts of *C. parvum* oocysts detected in the excreta and GI tracts of *H. schlegeli* clams after a single dose of oocysts at 6.67×10^4/clam. The data are means ± standard deviations for five replicates. The absence of bars indicates that the error was smaller than the symbol. (A) Percentage of *C. parvum* oocysts detected in feces. (B) Percentage of *C. parvum* oocysts in the GI tract. (C) Integrated recovery of oocysts in feces.

termined in the feces and GI tract contents of the clams after a single exposure to the oocysts showed that oocysts were rapidly ingested by the clams and excreted predominantly via the fecal route, as confirmed both microscopically (Fig. 1) and by PCR (Fig. 2). The pattern of oocyst excretion into the feces indicated two phases: a more rapid initial phase followed by a less rapid later phase, and 5 days after exposure, very few oocysts were detected in the feces. It was verified that the rate of oocyst intake by clams is rapid, and no oocysts were detected microscopically in the cistern water within 1 h after the start of exposure (data not shown). More than 80% of the oocysts were recovered in feces within 1 day after the start of exposure, and the total recovery of oocysts was around 93% within 4 to 5 days (Fig. 1A and C). The biological half-life ($t_{1/2}$) of the *C. parvum* oocysts in *H. schlegeli* clams was estimated to be about 12 h, shorter than that for *C. japonica* clams, as reported elsewhere (23). The pattern of decrease of oocysts in the GI tract contents was similar to that in the feces, as no oocysts were detected in the GI tract 4 days after the start of oocyst exposure (Fig. 1B).

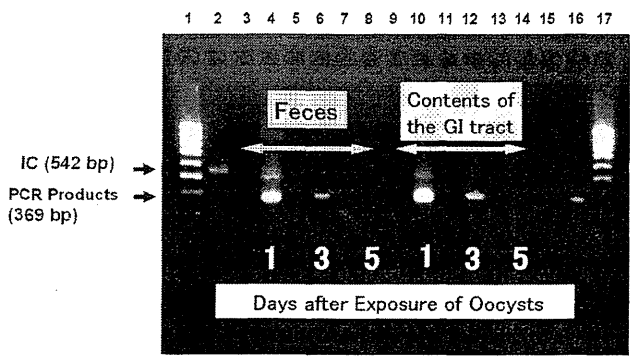

FIG 2 Ethidium bromide-stained 2.0% agarose gel showing amplification products obtained with TRAP-C2 primers from feces and GI tract samples from *H. schlegeli*. Lane 1, 100-bp molecular marker; lane 2, negative control (with IC); lane 4, fecal sample 1 day after exposure to oocysts; lane 6, fecal sample 3 days after exposure to oocysts; lane 8, fecal sample 5 days after exposure to oocysts; lane 10, GI tract sample 1 day after exposure to oocysts; lane 12, GI tract sample 3 days after exposure to oocysts; lane 14, GI tract sample 5 days after exposure to oocysts; lane 16, positive control; lane 17, 100-bp molecular marker.

The infectious activity of oocysts in the fecal samples, in terms of the rate of excystation, was around 75%, and there were no statistically significant differences between the excystation activities of fecal oocysts from clams and those of freshly prepared oocysts from mouse feces (*t* test, $\alpha = 5\%$ [data not shown]). Meronts were detected in HCT-8 cells 2 days after inoculation (Fig. 3), and there were no significant differences (*t* test, $\alpha = 5\%$) in the number of foci in infected HCT-8 cells between the clam fecal oocysts and those from mouse feces (data not shown). These results showed that oocysts were not digested by the clams and that oocysts in the feces retained their infectivity to host cells.

The changes in *C. parvum* oocyst concentration and cistern water turbidity with or without the clams or the feed (28 mg/liter) at 20°C are shown in Fig. 4A. The oocyst concentration and water turbidity without the clams showed very moderate reductions due to precipitation of the chow. On the other hand, the oocyst concentration in the presence of the clams, in the absence of chow, showed a slower reduction than when both the clams and chow were present. This suggested that the clams would hardly ingest plain oocysts as a natural food and that the observed slow reduction of oocyst numbers would have been due to ordinary gill breathing by the clam when not ingesting the chow.

On the other hand, for both the clams and the feed, the reductions in chow turbidity and oocyst concentration were significantly faster than in the former two cases (i.e., without the clam or the feed) (*t* test, $\alpha = 5\%$) and were very similar, showing synchro-

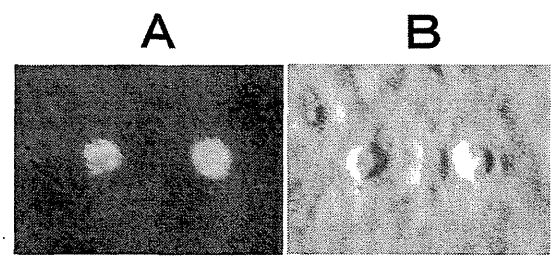

FIG 3 Photographs of developmental stages of *C. parvum* prepared from fecal samples of *H. schlegeli* clams in HCT-8 cells 2 days after inoculation. (A) Fluorescence micrograph of a field of meronts 2 days after inoculation with sporozoites prepared from a fecal sample. (B) Normarski interference-contrast photomicrograph of the corresponding field in panel A.

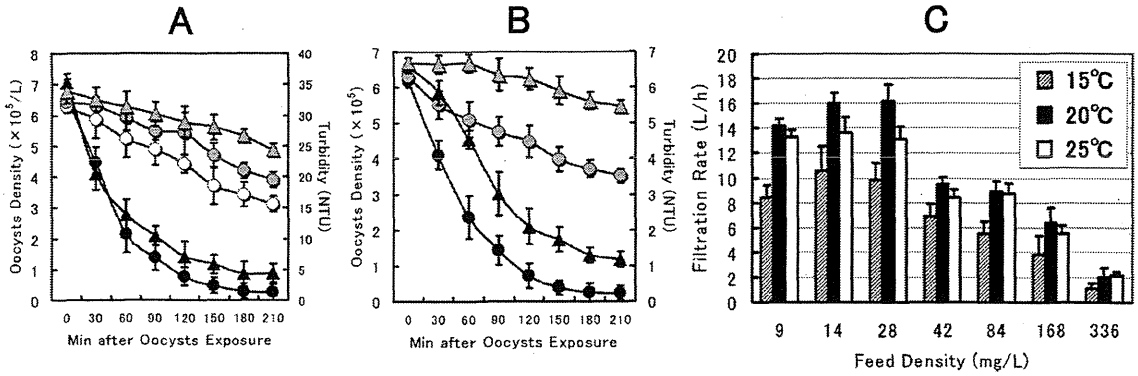

FIG 4 Reductions of *C. parvum* oocyst concentrations and water turbidity caused by the clams and rates of water filtration by the clams at various water temperatures and feed densities. Means and standard deviations are shown based on results from seven replicates. The absence of bars indicates that the error was smaller than the symbol. (A) Results obtained using laboratory water at 20°C. ●, oocyst density with both clams and feed (28 mg/liter); ○, oocyst density with clams but without feed; ◍, oocyst density without clams or feed; ▲, turbidity with both clams and feed; △, turbidity without clams but with feed. (B) Results obtained using final settling pond water at 20°C. ●, oocyst density with clams; ◍, oocyst density without clams; ▲, turbidity with clams; △, turbidity without clams. (C) Water filtration by clams at various water temperatures and feed densities. See Materials and Methods for details of calculation of the water filtration rate (in L/h).

nized reduction patterns. The faster gill breathing in the presence of the chow was considered attributable to an increased water filtration volume via the inhalant siphon when the clam sensed the presence of feed. We concluded that *H. schlegeli* would ingest *C. parvum* oocysts with the chow and that water filtration by the clams would translate into depletion of oocysts from the water.

The similar reductions of both the oocyst concentration and water turbidity caused by the clams in the water of the final settling pond are illustrated in Fig. 4B. It was clear that there were synchronized reductions in both oocyst density and the turbidity derived from impurities comprising the clam feed and various microorganisms. From these results, it was estimated that the clams would ingest any oocysts in the pond water and that neither the oocyst concentration nor turbidity would decrease in the absence of the clams.

On the other hand, the maximum water filtration rate by *H. schlegeli* (500 g) was between 10 liters/h (ca. 200 liters/day, at 15°C) and 16 liters/h (ca. 300 liters/day, at 20°C) at a chow density of 14 to 28 mg/liter, determined by measuring the initial turbidity reduction rates (Fig. 4C). These data clearly suggest that the clams would perform their filtration function at a moderate water temperature.

Clam fecal precipitation was observed in the presence of an artificial upward flow of 2.0 cm/s, the minimum realizable artificial flow rate, and about 100 times faster than that in the final settling pond. It was found that the feces of *H. schlegeli* clams settled to the bottom at a velocity of 1.0 to 1.5 cm/s against the upward flow. From this result, it was estimated that clam feces containing *C. parvum* oocysts would settle in the final settling pond, allowing them to be subjected to automated heat treatment.

Field survey in the sewage plant with *H. schlegeli* clams. The tests using fish revealed no unusual behaviors of the fish during the observation period (data not shown) and showed that 12 *H. schlegeli* clams with pearl cores were able to survive in the final settling pond with a mortality of 0% over a period of more than 3 years; 4 clams produced a total of six pearls during this period. These findings suggested that it was highly likely that *H. schlegeli* clams would survive in the pond for long periods, as pearls can only be produced in an environment that is stable and appropriate for the clam.

The results of analysis of the settling pond water showed that the temperature of the pond ranged from 15 to 24°C throughout the year and that the DO around the overflow trough ranged between 1.5 and 7.7 mg/liter, which is appropriate for the clams. However, the DO values at other points in the pond were often <1.0 mg/liter. The nitrogen values for ammonia and nitrites, which are harmful to gill-breathing organisms, reached high levels of 1.45 mg/liter and 2.30 mg/liter for a short period in August 2007, which were about 70 and 50 times higher, respectively, than those for the water in the laboratory. The total phosphorus was 0.20 to 0.50 mg/liter, 2 to 5 times higher than in the laboratory water, while the phosphorus in the form of soluble phosphate ions was maintained at a level of around 0.40 mg/liter, 20 times higher than the laboratory values. On the other hand, there were no remarkable differences in the concentrations of metals between the final settling pond water and the cistern water in the laboratory throughout the experimental period.

From these data, the biological and chemical qualities of the final settling pond water were considered to have no effects on the long-term survival of *H. schlegeli* clams.

The rise in the water level in the final settling pond was calculated as 18.6 m/day on the basis of the total drained water volume (1,600 m^3/day) and the water surface area (86 m^2) of the pond: this value would correspond to a water volume increase rate of 8.0 liters/h (0.02 cm/s) in a 100-cm^2 square column. Accordingly, it was estimated that if clams were placed at a density of 1 per 100 cm^2, they would theoretically filter the upward flow of the final settling pond with a water filtering ability of 10 to 16 liters/h throughout the year.

The data related to the reduction of water turbidity when using the clams are shown in Fig. 5, which presents the seasonal changes in the turbidity of water in the overflow trough. The water turbidity in the presence of *H. schlegeli* clams was shown to be around 35% lower than that of the control throughout the observation period. Significant differences in the rate of turbidity removal were found at 87% of the total data points relative to the controls

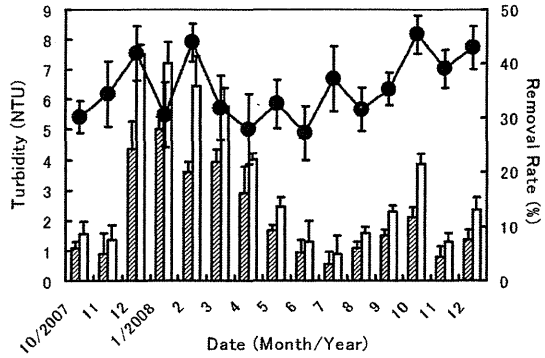

FIG 5 Time course of water turbidity and its rate of removal in the overflow trough water by *H. schlegeli* clams. The rate of turbidity (as a percentage) was calculated as described in the text. Means and standard deviations are shown based on results from five replicates. ▨, turbidity with clams; □, turbidity without clams (control); ●, rate of turbidity removal by clams.

(t test, $\alpha = 5\%$), proving that *H. schlegeli* clams filtered out the turbid components along with feed microbes in the pond water.

To study the filtration ability of *H. schlegeli* clams in more detail, in addition to the turbid components, the decreases in the densities of microorganisms trapped by the clams were monitored for 1 year. Classification and determination of microorganisms in the water of the final settling pond were carried out mainly for four phyla: Sarcomastigophora (classes Phytomastigophora, Zoomastigophorea, Lobosea, Filosea, Granuloreticulosea, and Heliozoea), Ciliophora (classes Peritrichia, Oligohymenophora, and Polyhymenophora), Aschelminthes (class Eurotatorea), and Protozoa (class Ciliatea). However, not all phyla were detected during the whole of the experimental period.

Data for both the seasonal densities of microorganisms stably observed throughout the year in the trough water and the rate of microbe removal by the clams are shown in Fig. 6. The microorganisms listed here were fed to the clams as natural chow and were also detected in the GI tracts of the clams. The rates of decrease of *Heterochromulina* sp. (class Phytomastigophora), *Gymnamoebia* sp. (class Lobosea), *Testacealobosia* sp. (class Lobosea), and *Vorticella* sp. (class Ciliatea) were around 41%, 61%, 50%, and 62%, respectively, and significant differences were detected in 73%, 80%, 80%, and 87% of total data points for each microbe, respectively (t test, $\alpha = 5\%$). Accordingly, these data confirmed that *H. schlegeli* clams are able to actively prey on microbes with *C. parvum* oocysts in the final settling pond water throughout the year, and the clams would consequently deplete 40 to 60% of the oocysts if practically applied to the sewage plant under the present conditions.

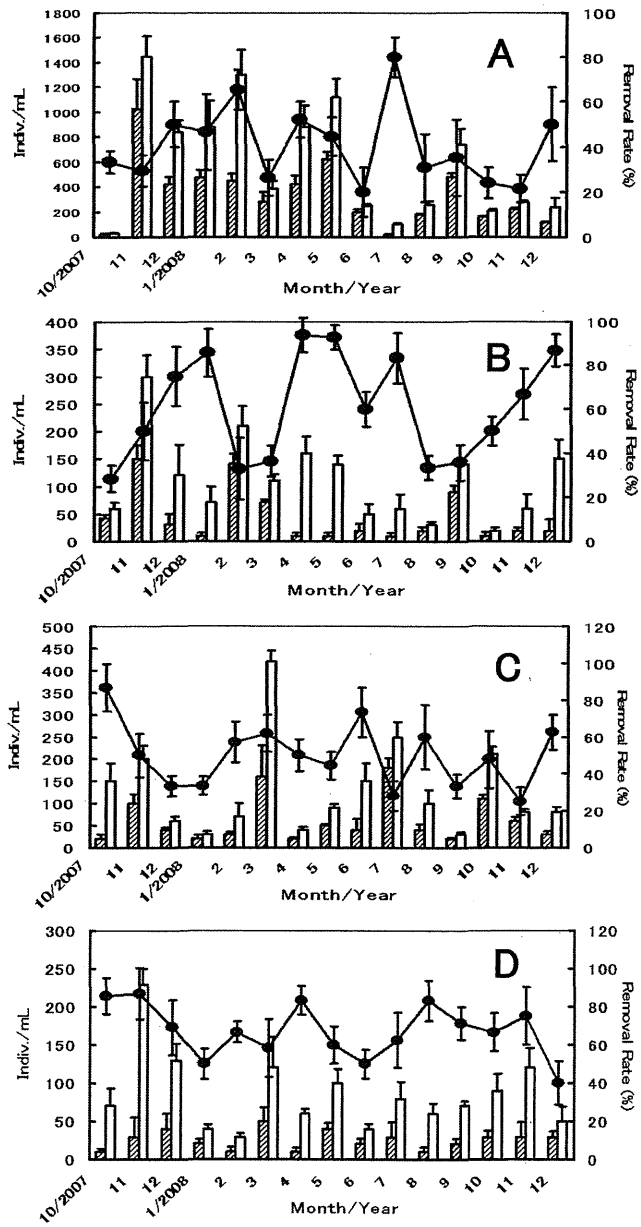

FIG 6 Time course of the density of microbes and their rates of removal from the overflow trough water by *H. schlegeli* clams. The rate of microbe removal (as a percentage) was calculated as described in the text. Means and standard deviations are shown based on results from five replicates. The absence of bars indicates that the error was smaller than the symbol. (A) *Heterochromulina* sp. (class Phytomastigophora); (B) *Gymnamoebia* sp. (class Lobesea); (C) *Testacealobosia* sp. (class Lobesea); (D) *Vorticella* sp. (class Ciliatea). ▨, density of microbes with clams present; □, density of microbes without clam present (control); ●, rate of microbe removal by the clams.

DISCUSSION

This study was conducted in order to develop a biological filtration system using the freshwater benthic pearl clam *Hyriopsis schlegeli* to deplete *Cryptosporidium* oocysts from contaminated sewage water. The biological trial was conducted with *H. schlegeli* clams placed in the final settling pond of a sewage plant, and we hypothesized that efficient removal of oocysts was possible based on data collected in preliminary investigations.

The preliminary trials involved maintaining the clams in the laboratory to examine their potential, including preservation of oocysts in the clam GI tracts and in feces, rates of water filtration, and the pattern of oocyst intake by the clams. The present trials produced results that accorded well with those obtained in the laboratory, and it was confirmed that the clams had considerable potential for filtration of a large water volume in the final settling pond throughout the year. It was established that oocysts trapped by the clams were not digested in the GI tract and were excreted predominantly in feces while retaining their ability to infect HCT-8 cells.